

# Infrared and optical invisibility cloak with plasmonic implants based on scattering cancellation

Mário G. Silveirinha,<sup>1,2</sup> Andrea Alù,<sup>1</sup> and Nader Engheta<sup>1,\*</sup>

<sup>1</sup>*Department of Electrical and Systems Engineering, University of Pennsylvania, Philadelphia, Pennsylvania 19104, USA*

<sup>2</sup>*Department of Electrical Engineering, Instituto de Telecomunicações, Universidade de Coimbra, 3030 Coimbra, Portugal*

(Received 18 March 2008; revised manuscript received 26 June 2008; published 11 August 2008)

In recent works, we have suggested that plasmonic covers may provide an interesting cloaking effect, dramatically reducing the overall visibility and scattering of a given object. While materials with the required properties may be directly available in nature at some specific infrared or optical frequencies, this is not necessarily the case for any given design frequency of interest. Here we discuss how such plasmonic covers may be specifically designed as metamaterials at terahertz, infrared, and optical frequencies using naturally available metals. Using full-wave simulations, we demonstrate that the response of a cover formed by metallic plasmonic implants may be tailored at will so that at a given frequency, it possesses the plasmonic-type properties required for cloaking applications.

DOI: [10.1103/PhysRevB.78.075107](https://doi.org/10.1103/PhysRevB.78.075107)

PACS number(s): 42.70.-a, 78.66.Sq, 41.20.Jb

## I. INTRODUCTION

In our previous works,<sup>1-5</sup> we have theoretically demonstrated that isotropic plasmonic materials with (relative) permittivity below unity may be used to drastically reduce the specific scattering of moderately sized obstacles. It was proven theoretically that such materials may behave as “antiphase” scatterers, which may effectively cancel out the dipolar radiation from the obstacle, inducing in this way electromagnetic invisibility. This phenomenon is possible because the polarization currents induced in a material with permittivity less than unity are in opposite phase with respect to the local electric field.

Recently, other groups have suggested alternative cloaking ideas<sup>6-11</sup> based on coordinate transformation theory, anomalous localized resonances, and other related concepts. Such configurations in general require anisotropic and/or inhomogeneous layers, and rely on the response of resonant metamaterials and artificial magnetism. On the contrary, the transparency phenomenon proposed by our group<sup>1</sup> simply requires uniform plasmonic materials with an isotropic response. Moreover, this transparency mechanism does not rely on a resonant effect, and so it is less affected by losses and may have good tolerance with respect to changes in the geometrical or material parameters of the involved objects.<sup>2</sup>

While isotropic plasmonic materials with the required electromagnetic properties may be readily available in nature at certain specific IR or optical frequencies,<sup>12</sup> in general one may need to synthesize these materials as metamaterials to operate with the required electromagnetic properties at a desired frequency. Such ideas were explored in our previous work,<sup>5</sup> where we have effectively demonstrated at microwaves how it may be possible to emulate the behavior of low or negative permittivity materials in cloaks by using parallel-plate metallic implants embedded in a dielectric host. Namely, we have shown how to effectively design metamaterial cloaks using perfectly electric conducting (PEC) implants. In this sense, we had to properly take into account both interface effects and actual granularity of the structured material, demonstrating numerically that these metamaterial cloaks may indeed provide a drastic scattering reduction,

analogous to their homogeneous ideal models.

The goal of the present study is to extend the concepts introduced in Ref. 5 to the IR and visible domains, properly taking into account the fact that at terahertz, IR, and optical frequencies, metals have finite conductivity, well modeled to a good approximation, as Drude plasmas. We derive some simple design formulas for a class of novel metamaterial cloaks that operate at infrared and optical frequencies based on plasmonic parallel-plate implants in a dielectric host, and we demonstrate with full-wave simulations how such parallel-plate metallic covers may effectively reroute the incoming light and induce a cloaking effect at the desired IR or optical frequency.

## II. METAMATERIAL DESIGN

The cloaking effect described in Ref. 1 exploits the negative polarizability provided by scatterers made of materials with  $\epsilon$  negative (ENG) or  $\epsilon$  near zero (ENZ) ( $\epsilon$  representing the material permittivity). For typical designs,<sup>1-5</sup> the required value of the (real part of the) permittivity  $\epsilon_c$  of the plasmonic cover lies in the range  $-10\epsilon_0 < \text{Re}\{\epsilon_c\} < 0.5\epsilon_0$ , with  $\epsilon_0$  being the free-space permittivity. Since noble metals behave essentially as ENG materials at infrared and optical frequencies, they may be directly used for cloaking purposes.<sup>1</sup> A problem, however, may arise in that for frequencies one or two decades below the plasma frequency of the material of interest, the (real part of) permittivity of such metals, even though negative, may have an absolute value orders of magnitude larger than the permittivity of vacuum. For example, following the experimental data tabulated in Ref. 13 at IR frequencies, silver may be well characterized by a Drude model  $\epsilon_{Ag}/\epsilon_0 = \epsilon_\infty - \omega_p^2/\omega(\omega + i\Gamma)$ , with  $\epsilon_\infty = 5.0$ ,  $\omega_p = 2\pi \times 2175$  [THz], and  $\Gamma = 2\pi \times 4.35$  [THz]. This yields  $\epsilon_{Ag} \approx 470(-1 + 0.04i)\epsilon_0$  at 100 THz, which is 2 orders of magnitude larger than the typical values required for cloaking applications.

To overcome this inconvenience, mimicking our microwave setup<sup>5</sup> we suggest to embed silver implants in a dielectric region (with positive  $\epsilon$ ), so that the resulting composite

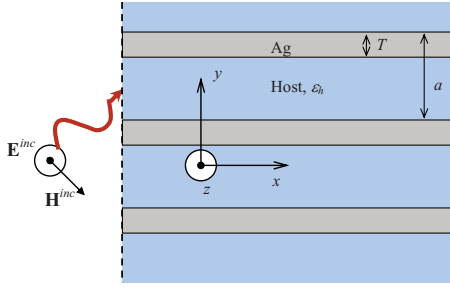


FIG. 1. (Color online) Geometry of a truncated (semi-infinite) planar composite material formed by a periodic array of nanolayers of silver embedded in a dielectric host. The truncated sample is illuminated by an incoming  $TE^x$  plane wave.

material has a tailored electromagnetic response suitable for cloaking.

The geometry of the proposed layered structure in its planar version is depicted in Fig. 1. It consists of a periodic array of planar silver slabs with permittivity  $\epsilon_{Ag}$  inserted in a dielectric host material with permittivity  $\epsilon_h$ . The thickness of each silver layer is  $T$  and the lattice constant is  $a$ . The effective response of such metamaterial for propagation in the  $x$ - $y$  plane with electric field along  $z$  may be readily characterized using the well-known dispersion characteristic of  $E$ -polarized Floquet modes:<sup>14</sup>

$$\begin{aligned} \cos(k_y a) &= \cos(k_{y,2} T) \cos[k_{y,1} (a - T)] \\ &- \frac{1}{2} \left( \frac{k_{y,1}}{k_{y,2}} + \frac{k_{y,2}}{k_{y,1}} \right) \sin(k_{y,2} T) \sin[k_{y,1} (a - T)], \end{aligned} \quad (1)$$

where  $\mathbf{k} = (k_x, k_y, 0)$  is the wave vector of the Floquet mode,  $\omega$  is the angular frequency of operation,  $k_{y,1} = \sqrt{\epsilon_h \mu_0 \omega^2 - k_x^2}$ , and  $k_{y,2} = \sqrt{\epsilon_{Ag} \mu_0 \omega^2 - k_x^2}$ . For a fixed frequency, the structured material supports an infinite countable number of electromagnetic modes with propagation constants along  $x$  given by  $k_x^{(n)} = k_x^{(n)}(\omega, k_y)$ ,  $n = 0, 1, 2, \dots$ , which can be calculated from Eq. (1). It is simple to verify that for long wavelengths all the electromagnetic modes are attenuated ( $\text{Im}\{k_x^{(n)}\} \neq 0$ ), even in the absence of losses. To homogenize the structured metamaterial, we will characterize the least attenuated electromagnetic mode (associated with the index  $n=0$ ). In this work, we are particularly interested in propagation along the  $x$  direction ( $k_y=0$ ). In such situation, the composite material is described to a good approximation by an effective permittivity given by the formula:

$$\epsilon_{\text{eff}} = \frac{(k_x^{(0)}(\omega)|_{k_y=0})^2}{(\omega/c)^2}. \quad (2)$$

Obviously, the effective permittivity depends not only on the permittivity of the components, but also on their volume fractions. Thus, by adjusting  $T$  and  $a$  it is possible to tune the response of the material according to our needs. This is illustrated in Fig. 2, where we plot  $\epsilon'$  and  $\epsilon''$  with  $\epsilon_{\text{eff}} = \epsilon_0(\epsilon' - i\epsilon'')$ , as a function of frequency for a structured material formed by silver nanolayers with thickness  $T = 13.5$  nm, spaced by  $a = 360$  nm, and embedded in a dielec-

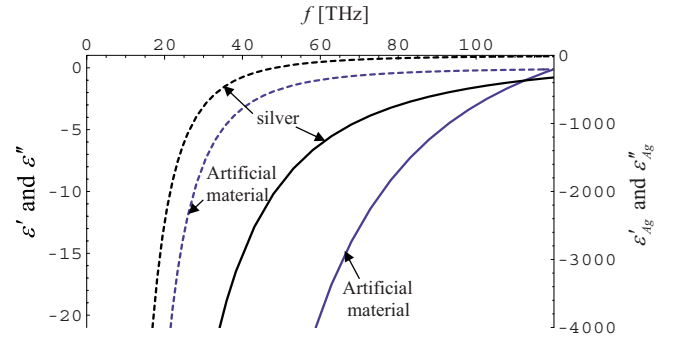


FIG. 2. (Color online) Permittivity as a function of frequency: Blue lines (associated with left-hand side scale): structured material; Black lines (associated with right-hand side scale): silver. The artificial material is formed by silver slabs with thickness  $T = 0.0374a$  which are spaced by  $a = 360$  nm and embedded in a host material with  $\epsilon_h = 6.5$ .

tric material with permittivity  $\epsilon_h = 6.5\epsilon_0$  [SiC has similar properties around 100 THz (Ref. 15)]. These values were chosen to obtain  $\text{Re}\{\epsilon_{\text{eff}}\} = -3.0\epsilon_0$  at 100 THz, and they will be used in the following to design a plasmonic metamaterial cloak. In the same graphic we have also plotted (using a different scale) the permittivity of silver<sup>13</sup> to show how dramatically different the two dispersions are. Indeed, the permittivity of silver is 2 orders of magnitude larger than the one of the composite medium.

The description of the composite material using the dielectric function (2) relies on the assumption that the effect of the higher-order evanescent modes (associated with the indices  $n = 1, 2, \dots$ ) is negligible. In general such approximation is fairly accurate in the long-wavelength limit, especially if the thickness  $L$  of the considered metamaterial slab (measured along  $x$ ) is significantly larger than the lattice constant. However, when the metamaterial slab is relatively thin and  $L$  is comparable to  $a$ , interface effects become increasingly important, and the effect of higher-order modes, even though small, is sufficient to detune the response of the material. These effects have been carefully analyzed in our previous work<sup>5</sup> for the case of PEC slabs at microwave frequencies, where it was demonstrated that the higher-order modes could modify the expected response of the composite material in several scenarios of interest.

Nevertheless, it is possible to take into account the granularity of the composite material and the existence of higher modes in a straightforward manner. The idea is to introduce “virtual interfaces” that describe the effective boundaries of the composite material. These virtual interfaces are displaced at a distance  $\delta$  with respect to the actual physical interface of the layered material. This concept, first explored in Ref. 5, is illustrated in the inset of Fig. 3. The proper choice of  $\delta$  may indeed allow, also in this scenario, to describe a metamaterial slab with thickness  $L - 2\delta$  adjoined by two dielectric layers with permittivity  $\epsilon_h$  and thickness  $\delta$  effectively as a continuous medium with thickness  $L$  and dielectric function given by Eq. (2). The thickness  $\delta$  of these dielectric “gaps” depends mostly on the lattice constant  $a$  and on the properties of the metal. For example, for vanishingly thin PEC plates,  $\delta \approx 0.1a$ .<sup>5</sup> In the more general present case for which the

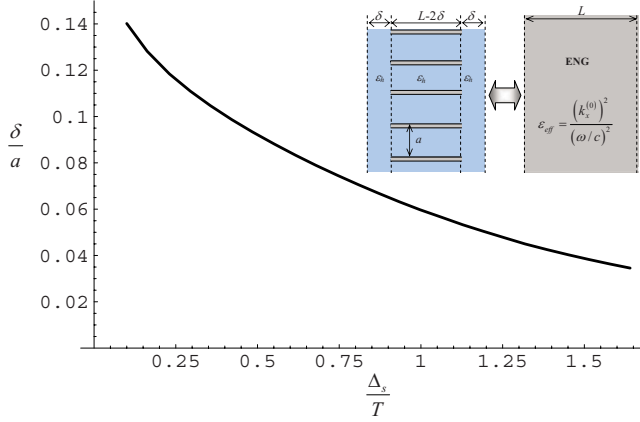


FIG. 3. (Color online) Virtual interface position  $\delta$  as a function of the skin depth of the metal  $\Delta_s$  at 100THz. The parameters  $T$ ,  $a$ , and  $\epsilon_h$  are as in Fig. 2. The inset illustrates the equivalence between a composite material slab with two adjoining dielectric layers with thickness  $\delta$ , and a continuous material described by the dielectric function (2).

thickness and the conductivity of the metallic plates are finite,  $\delta$  may be calculated using formula (A14) in the Appendix. To illustrate the dependence of  $\delta$  with the properties of the metal, in Fig. 3 we plot  $\delta$  as a function of the skin-depth  $\Delta_s$  of the metal at 100 THz. The composite material is characterized by the same parameters  $a$ ,  $T$ , and  $\epsilon_h$  as in Fig. 2, and the permittivity of the metallic layers  $\epsilon_m$  is assumed to be the free parameter (the skin depth is given by  $\Delta_s = 1/\omega\sqrt{-\epsilon_m\mu_0}$ ; for silver  $\Delta_s = 1.64T$  at the considered frequency). It is seen that  $\delta$  depends appreciably on  $\Delta_s$  and decreases when  $\Delta_s$  increases, or equivalently as the conducting properties of the metal deteriorate. For example, when the metal is made of silver we get  $\delta = 0.035a$ .

### III. CLOAK DESIGN

Having introduced the necessary homogenization concepts, we are now ready to design a plasmonic metamaterial with the desired permittivity at IR or optical frequencies and apply it to a cloak. Consider a dielectric cylindrical object with permittivity  $\epsilon_{\text{obj}} = 3.0\epsilon_0$  at 100 THz and diameter  $2R = 0.76 \mu\text{m} = 0.25\lambda_0 = 0.44\lambda_{\text{diel}}$  ( $\omega 2R/c = 1.6$  at 100 THz). To reduce its visibility and scattering, we may design a suitable plasmonic cloak. Assuming that the cloak permittivity is  $\epsilon_c = -3\epsilon_0$ , our theory<sup>1-5</sup> shows that the scattering width of the cloaked system is drastically reduced when the cloak radius is equal to  $R_c = 1.40R$ .

Inspired by the planar metamaterial configuration of Fig. 1 and by our work at microwaves,<sup>5</sup> we design a cylindrical cloak as shown in the inset of Fig. 4. The cloak is formed by  $N=8$  silver implants with thickness  $T$ , oriented along the radial direction, and uniformly spaced along the azimuthal direction.<sup>16</sup> The metallic implants are embedded in SiC, which is characterized by  $\epsilon_h \approx 6.5\epsilon_0$  at 100 THz (Ref. 15) (for simplicity, in this work we will neglect the frequency dependence of the permittivity of SiC). The effective permittivity of the proposed cloak may be estimated as in Eq. (2).

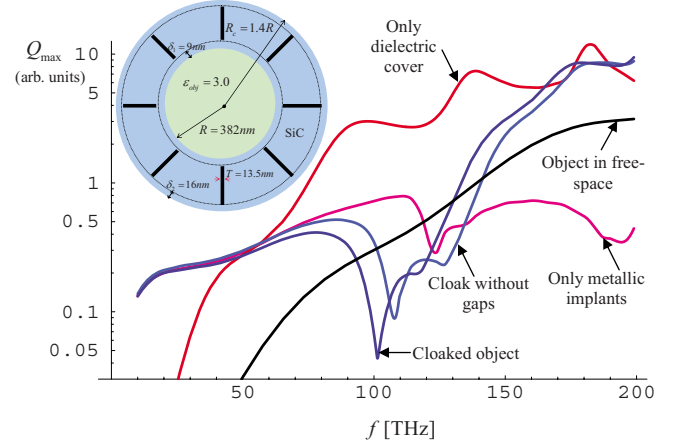


FIG. 4. (Color online) Peak in the scattering width  $Q$  (normalized to arbitrary units) as a function of frequency, for different scenarios of interest. The inset represents a combined object-cloak system (the different parts of the cloak are not drawn to scale).

However, it is noted that in the configuration shown in the inset of Fig. 4 the spacing between the plates is not uniform, and strictly speaking it depends on the radial coordinate:  $a = a(r) = 2\pi r/N$ . This implies that in general the effective permittivity of cloak is also a weak function of  $r$ .<sup>5</sup> In principle, it is possible to design a cloak with uniform permittivity by varying the thickness of the implants  $T$  as a function of  $r$  so that the effective permittivity would be independent of the radius. However, this solution may be challenging from a technological point of view. It is much simpler to assume that the thickness  $T$  is constant and replace  $a$  by its average value  $a_{\text{med}} = \pi(R+R_c)/N$  in the design formulas for the planar geometry. Proceeding in this way, we obtain  $\omega a_{\text{med}}/c = 0.75$ . Feeding this value to Eq. (2) and imposing that  $\text{Re}\{\epsilon_c\} = -3\epsilon_0$ , it is found that the required thickness for the metallic plates is  $T = 0.0374 a_{\text{med}} = 13.5 \text{ nm}$ . The corresponding effective permittivity is  $\epsilon_c = \epsilon_0(-3.0 + 0.2i)$  at 100 THz.

As depicted in the inset of Fig. 4, we introduce two small SiC cylindrical shells with thicknesses  $\delta_1$  and  $\delta_2$  at the interfaces of the structured material with the object and with the air region, respectively. As described before, these shells are necessary to fully take into account the effects of higher-order modes and of the granularity of the artificial material. Following the results in the Appendix, it may be verified that the cloak design requires  $\delta_1 = 0.030a(R)$  and  $\delta_2 = 0.039a(R_c)$ , which yields  $\delta_1 = 9 \text{ nm}$  and  $\delta_2 = 16 \text{ nm}$ .

Using the full-wave electromagnetic simulator CST Microwave Studio<sup>TM</sup>,<sup>17</sup> we have calculated the variation of the peak in scattering width  $Q_{\text{max}}$  of the combined object-cloak system vs frequency, as reported in Fig. 4 for different configurations of interest. The system is always illuminated by a plane wave that propagates along the  $x$  direction and has electric field parallel with the axis of the cylinder ( $z$  direction). It is seen that when the object stands alone in free space its scattering width (black line in Fig. 4) increases monotonically with its electrical size, consistent with what one may intuitively expect. Quite distinctly, however, when the object is covered with the metamaterial cloak (dark blue

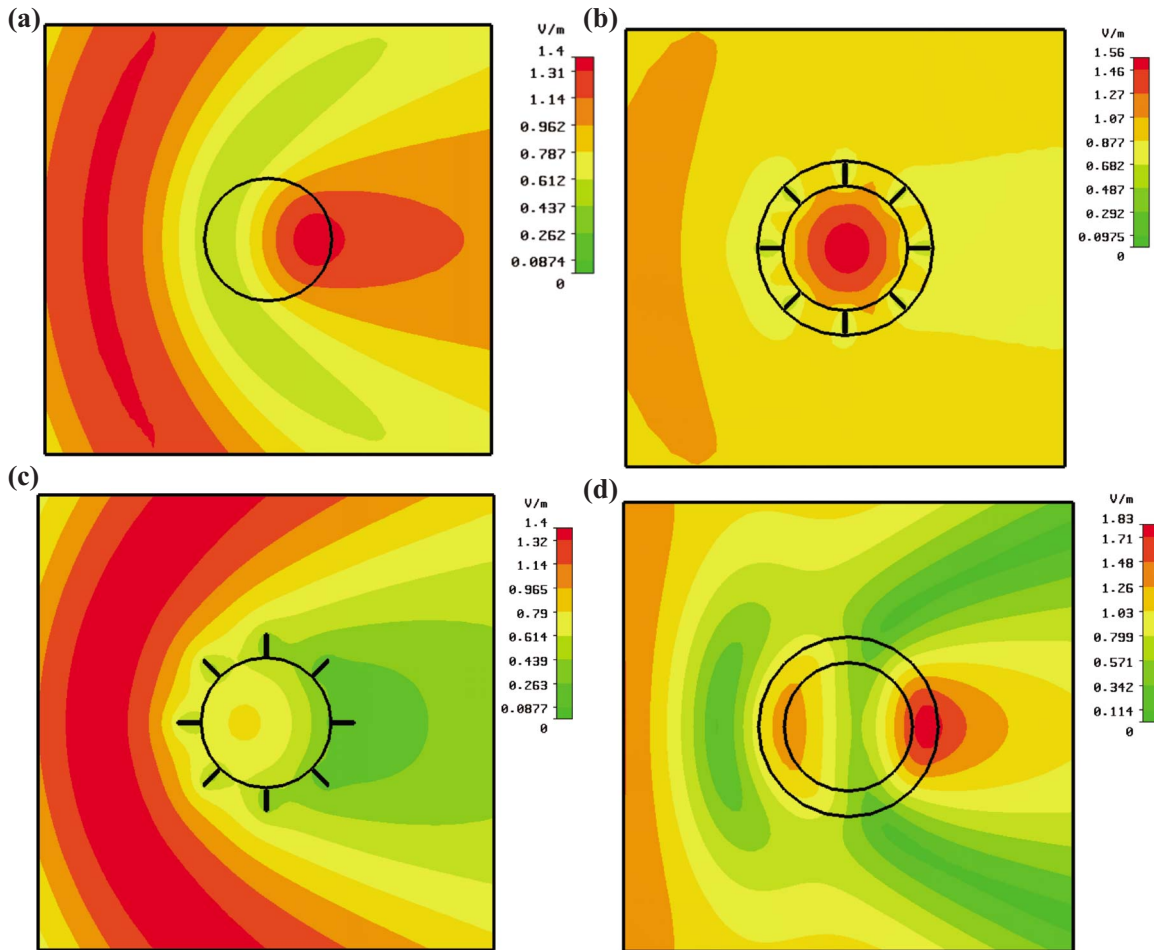


FIG. 5. (Color online) Amplitude of the electric field for an object with (a) no cloak, (b) metamaterial cloak, (c) cloak with only metallic implants, and (d) dielectric cloak.

line in Fig. 4), the scattering width of the combined system is greatly reduced around the design frequency of 100 THz, despite the fact that the physical size of the system has increased when the cloak is added. Such property stems from the plasmonic-like properties of the metamaterial cloak, which ensure that the polarization currents induced in the cloak are out of phase with the polarization currents induced in the object, effectively eliminating the dipolar-type component of the scattered field.<sup>1-5</sup> This property is further supported by the simulations obtained for the cases in which the object is just covered with SiC (red line in Fig. 4), or surrounded by silver implants (pink line in Fig. 4). In fact, in these two scenarios the scattering width is greatly enhanced as compared to the uncloaked case. Finally, we have also plotted the scattering width of the system when virtual interfaces are ignored and  $\delta_1$  and  $\delta_2$  are set equal to zero (light blue line in Fig. 4). It is seen that in this last scenario the overall response of the system is detuned, even though  $Q_{\max}$  may still become significantly lower than the corresponding value for an uncloaked object around the design frequency. We have also verified that the response of the metamaterial cloak (with the virtual interfaces) mimics very closely the response of an equivalent continuous material cloak with permittivity given by Eq. (2) (not shown here for sake of brevity).

To further support our theory, the amplitude of the  $z$  component of the electric field is reported in Fig. 5 for the different configurations discussed above. When the object is cloaked with the metamaterial [panel (b) of Fig. 5], the field in the air region is nearly uniform, showing that even in the near-field region the scattered field is very weak. Quite differently, for the other configurations in which the object is either uncloaked [panel (a)], or cloaked with only metallic implants or only SiC [panels (c) and (d), respectively], the field in the air region is highly nonuniform due to strong dipolar scattering from the system. Since the scattered field of the cloaked system is very weak in the near field at the design frequency, the coupling between an arbitrary number of such cloaked objects would be negligible and their combined scattering width would stay very small, even if the objects are closely spaced, consistent with our findings for the case of continuous material cloaks.<sup>3</sup> This situation is reported in Fig. 6, where we show the transmission coefficient  $\tau$  as a function of frequency, when a plane wave propagating along the  $x$  direction illuminates a periodic array of cloaked objects arranged along the  $y$  axis, as depicted in the figure inset. Independently from the distance  $d$  between the cloaked objects, the periodic array is effectively transparent to radiation around 100 THz, even when  $d$  is as small as  $1.1 \times 2R_c$ . Moreover, following the results in Ref. 4 we may envision

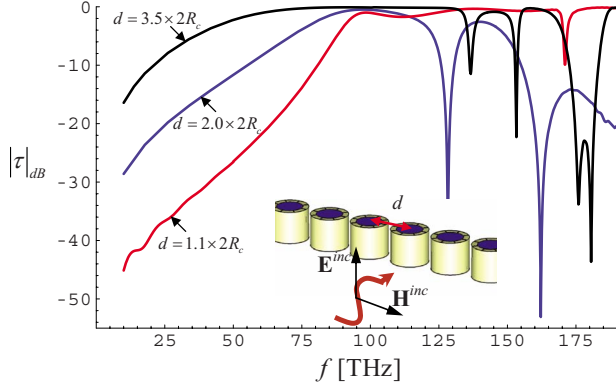


FIG. 6. (Color online) Amplitude of the transmission coefficient (in dBs) for an array of cloaked objects illuminated by a plane wave (normal incidence). The distance between adjacent objects is  $d$ . The geometry is depicted in the inset.

the possibility of using different metamaterial covers to operate the cloak simultaneously at different frequencies.

#### IV. CONCLUSIONS

We have demonstrated the possibility of designing realistic metamaterials that achieve an effective plasmonic-type response at selected infrared and optical frequencies for which natural materials with the same characteristics may not be readily available. The proposed design fully takes into account the finite conductivity of metals and the granularity of the artificial materials. Full-wave simulations have demonstrated that such metamaterial cloaks may drastically reduce the scattering width of a given object or array of objects at the mid-IR band. Similar results may be obtained at other infrared or optical frequencies. This suggests exciting potentials for metamaterials with a plasmonic-type response.

#### ACKNOWLEDGMENTS

This work is supported in part by Fundação para Ciência e a Tecnologia under Project No. PDTC/EEA-TEL/71819/2006.

#### APPENDIX

In this Appendix, we calculate the displacement  $\delta$  of the virtual interfaces with respect to the physical interfaces. To this end, first we will obtain the reflection coefficient for a plane wave that illuminates a semi-infinite structure formed by a periodic array of stacked plasmonic slabs. The geometry of the problem is shown in Fig. 1. It is assumed that the incident electric-field vector is along the  $z$  direction, and has amplitude  $E_z^{\text{inc}}$  at the interface. For simplicity, the host material is assumed to be air.

The main idea for solving this electromagnetic problem has been proposed in Refs. 18 and 19 and it uses the property that the transmitted field (in the region  $x > 0$ ) may be written in terms of the electromagnetic modes  $\mathbf{E}_n(\mathbf{r}; \mathbf{k}_n)$  ( $n=0, 1, 2, \dots$ ) supported by the associated unbounded periodic material,

$$\mathbf{E}(\mathbf{r}) = \sum_n c_n \mathbf{E}_n(\mathbf{r}; \mathbf{k}_n), \quad x > 0, \quad (\text{A1})$$

where  $c_n$  are the unknown coefficients of the expansion and  $\mathbf{k}_n = k_x^{(n)} \hat{\mathbf{u}}_x + k_y \hat{\mathbf{u}}_y$  is the wave vector associated with the mode  $\mathbf{E}_n(\mathbf{r}; \mathbf{k}_n)$ . Since in a scattering problem the component of the wave vector parallel to the interface is preserved, the component  $k_y$  is completely determined by the angle of incidence  $\theta_i$  of the incoming plane wave:  $k_y = (\omega/c) \sin \theta_i$ . On the other hand,  $k_x^{(n)}$  depends on the considered mode and is both a function of frequency  $\omega$  and of  $k_y$ . Since the periodic material is invariant to translations along the  $x$  and  $z$  directions and the incoming wave propagates in the  $x$ - $y$  plane, it is clear that  $\mathbf{E}_n(\mathbf{r}; \mathbf{k}_n)$  may be assumed of the form,

$$\mathbf{E}_n(\mathbf{r}; \mathbf{k}_n) = E_z^{(n)}(y) e^{+ik_x^{(n)} x} \hat{\mathbf{u}}_z, \quad (\text{A2})$$

where the propagation constants  $k_x^{(n)}$  ( $n \geq 0$ ) may be calculated numerically by solving Eq. (1) with respect to  $k_x$  for given  $\omega$  and  $k_y$ . For example, for vanishingly thin PEC slabs, the propagation constants  $k_x^{(n)}$  are given by  $k_x^{(n)} = i \sqrt{[(n+1)\pi/a]^2 - (\omega/c)^2}$ . For a fixed frequency and for  $n$  sufficiently large  $k_x^{(n)}$  is complex imaginary, which is consistent with the fact that the number of propagating Floquet modes supported by the unbounded crystal is finite.

Using the results of Refs. 18 and 19, formula (A2), and taking into account that the problem is two dimensional, it may be proven that the unknown coefficients  $c_n$  satisfy the following infinite linear system of equations:

$$E_z^{\text{inc}} \delta_{l,0} = \sum_{n=0}^{\infty} A_{n,l} \frac{1}{\gamma_l + ik_x^{(n)}}, \quad l = 0, \pm 1, \pm 2, \dots, \quad (\text{A3})$$

where  $\gamma_l = \sqrt{(k_y + 2\pi l/a)^2 - (\omega/c)^2}$  and

$$A_{n,l} = \frac{c_n}{2\gamma_0} \left( \frac{\omega}{c} \right)^2 q_n \left( k_y + \frac{2\pi l}{a} \right),$$

with

$$q_n(k'_y) = \frac{1}{a} \int_{\text{diel.}} (\varepsilon_r - 1) E_z^{(n)}(y) e^{-ik'_y y} dy. \quad (\text{A4})$$

In the above,  $\varepsilon_r$  represents the relative permittivity of the plasmonic slabs and the integral in the definition of  $q_n(k'_y)$  is calculated over the plasmonic slab in the unit cell. Similarly, following Refs. 18 and 19 it may be proven that the amplitude of the reflected electric field at the interface  $E_z^{\text{ref}}$  verifies:

$$E_z^{\text{ref}} = - \sum_{n=0}^{\infty} A_{n,0} \frac{1}{-\gamma_0 + ik_x^{(n)}}. \quad (\text{A5})$$

Hence, it is possible to compute the reflected field by: (i) solving the infinite linear system (A3) with respect to the unknowns  $c_n$  [notice that the entries of the linear system are written in terms of  $k_x^{(n)}$  and  $E_z^{(n)}(y)$ , which may be (numerically) determined by computing the eigenmodes of the associated unbounded periodic stratified material]; (ii) substituting the calculated  $c_n$  into Eq. (A5) to obtain  $E_z^{\text{ref}}$ . This procedure yields the exact reflection coefficient, but requires, manifestly, significant computational efforts. It is however

possible to considerably simplify the problem by making some reasonable assumptions. In fact, let us suppose that  $T \ll a$ , i.e., the thickness of the plasmonic slab is much smaller than the lattice constant. In such conditions it is valid to make the approximation  $q_n(k_y + 2\pi/al) \approx q_n(k_y)$  for the range of integers  $l$  for which the term  $e^{-i2\pi l/ay}$  is approximately constant over the plasmonic material, i.e., for  $(2\pi/a)lT \ll \pi$ . It is clear that the thinner the plasmonic slab, the better is this approximation. Also the approximate identity is more accurate for smaller values of  $l$ , which correspond to the lowest-order Fourier harmonics (which are the most important, since the higher-order evanescent harmonics are in principle weakly excited). Using this approximation, it follows that  $A_{n,l} \approx A_{n,0}$ , and thus the infinite linear system (A3) can be rewritten as:

$$E_z^{\text{inc}} \delta_{m,0} = \sum_{n=0}^{\infty} A_{n,0} \frac{1}{z_m - p_n}, \quad m = 0, 1, 2, \dots, \quad (\text{A6})$$

where we defined  $p_n = -ik_x^{(n)}$  ( $n=0, 1, 2, \dots$ ) and  $z_m$  ( $m=0, 1, 2, \dots$ ) such that  $z_0 = \gamma_0$  and

$$z_{2l} = \gamma_{-l}; \quad z_{2l-1} = \gamma_l \quad (l = 1, 2, \dots). \quad (\text{A7})$$

In this scenario, following the ideas of Refs. 18–21 the solution  $A_{n,0}$  ( $n=0, 1, 2, \dots$ ) of the system (A6) may be calculated in closed analytical form. To simplify the discussion we will truncate the infinite series in Eq. (A6) so that it reduces to the sum of a finite number ( $N$ ) of terms. This is clearly possible on physical grounds since, as mentioned above, the higher-order evanescent electromagnetic modes are weakly excited. Thus, Eq. (A6) becomes:

$$E_z^{\text{inc}} \delta_{m,0} = \sum_{n=0}^N A_{n,0} \frac{1}{z_m - p_n}, \quad m = 0, 1, 2, \dots, N. \quad (\text{A8})$$

Consider now the auxiliary complex function  $f(w)$  ( $w$  is the complex variable) given by:

$$f(w) = \frac{C}{1 - w/p_0} \prod_{n=1}^N \frac{1 - w/z_n}{1 - w/p_n}, \quad (\text{A9})$$

where the constant  $C$  is calculated so that  $f(z_0) = E_z^{\text{inc}}$ . It is clear that  $f(w)$  has zeros at the points  $w = z_m$  ( $m=1, 2, \dots$ ) and poles at the points  $w = p_n$  ( $n=0, 1, 2, \dots$ ). In addition  $f(w)$  converges to zero at the same rate as  $1/w$ , as  $w$  goes to infinity. In particular, applying the residues theorem it is simple to verify that

$$f(w) = \sum_{n=0}^N \frac{\text{Res}(f)|_{w=p_n}}{w - p_n}, \quad (\text{A10})$$

where  $\text{Res}(f)|_{w=p_n}$  is the residue of  $f(w)$  at the pole  $p_n$ . However, since  $f(z_0) = E_z^{\text{inc}}$  and  $f(z_m) = 0$  ( $m=1, 2, \dots$ ), it is evident—comparing Eq. (A8) to Eq. (A10)—that the solution of the truncated infinite linear system is given by  $A_{n,0} = \text{Res}(f)|_{w=p_n}$ , which may be calculated explicitly using Eq. (A9). This yields the exact solution of the truncated linear system for arbitrary  $N$ . In particular, we note that Eqs. (A5) and (A8) are equivalent to  $E_z^{\text{inc}} \delta_{m,0} = f(z_m)$ ,

$m=0, 1, 2, \dots, N$ , and  $E_z^{\text{ref}} = -f(-z_0)$ , respectively, and so the reflection coefficient is given by:

$$\rho \equiv \frac{E_z^{\text{ref}}}{E_z^{\text{inc}}} = -\frac{f(-\gamma_0)}{f(\gamma_0)} = -\frac{p_0 - \gamma_0}{p_0 + \gamma_0} \prod_{n=1}^N \frac{p_n - \gamma_0 z_n + \gamma_0}{p_n + \gamma_0 z_n - \gamma_0}. \quad (\text{A11})$$

In order to obtain the solution of the infinite linear system (A6), we may now let  $N$  go to infinity. It may be verified that, for the infinite product in Eq. (A9) to converge for  $N \rightarrow \infty$ , it is sufficient that the sequences of poles and zeros grow to infinity,  $|z_n| \rightarrow \infty$  and  $|p_n| \rightarrow \infty$ , and in addition that  $\sum_n |1/z_n - 1/p_n| < \infty$ .<sup>18</sup> The latter condition is verified when, for  $n$  sufficiently large, the poles and the zeros alternate in the real line.<sup>18</sup> It may be verified that if the poles and zeros of the problem are ordered in such a way that  $\text{Re}\{p_n\}$  and  $\text{Re}\{z_n\}$  are monotonically increasing sequences, the convergence of the infinite product is ensured.

By letting  $N \rightarrow \infty$ , Eq. (A11) can be rewritten as

$$\rho = \rho_e e^{2\gamma_0 \delta}, \quad \rho_e = -\frac{-ik_x^{(0)} - \gamma_0}{-ik_x^{(0)} + \gamma_0}, \quad (\text{A12})$$

where  $\rho_e$  is the reflection coefficient that would be obtained under the hypothesis that the effect of all higher-order modes is negligible and the scattering problem can be described using only the fundamental mode. The factor  $e^{2\gamma_0 \delta}$  is a correction term (which takes into account the effect of higher-order modes) given by:

$$e^{2\gamma_0 \delta} = \prod_{n=1}^{\infty} \frac{p_n - \gamma_0 z_n + \gamma_0}{p_n + \gamma_0 z_n - \gamma_0}. \quad (\text{A13})$$

Notice that  $\gamma_0$  is complex imaginary:  $\gamma_0 = -i\sqrt{(\omega/c)^2 - k_y^2}$ . It is simple to verify that in the long-wavelength limit and in case of negligible losses, the zeros  $z_n$  and the poles  $p_n$  ( $n \geq 1$ ) are all real valued. Thus, it is evident that in such conditions  $|e^{2\gamma_0 \delta}| = 1$ , and thus the parameter  $\delta$  is real valued. As explained in our previous work,<sup>5</sup> the parameter  $\delta$  determines the displacement of “the virtual interface” with respect to the physical interface. From the point of view of an incoming wave, the stratified semi-infinite material behaves effectively as a continuous material, characterized by the effective permittivity obtained from the slope of the dispersion characteristic of the fundamental mode, being the effective interface with air positioned at the plane  $x = -\delta$  instead of at the physical interface ( $x=0$ ). From Eq. (A13), it is clear that  $\delta$  is given by:

$$\delta = \frac{1}{|\gamma_0|} \sum_{n=1}^{\infty} \arctan\left(\frac{|\gamma_0|}{z_n}\right) - \arctan\left(\frac{|\gamma_0|}{p_n}\right). \quad (\text{A14})$$

In general,  $\delta$  is a function of frequency  $\omega$ , wave vector  $k_y$ , and of course of the thickness and permittivity of the dielectric slabs. For normal incidence,  $z_n$  is such that  $z_{2l} = z_{2l-1} = \sqrt{(2\pi l/a)^2 - (\omega/c)^2}$  ( $l=1, 2, \dots$ ), and  $p_n = -ik_x^{(n)}$  ( $n \geq 1$ ) are the attenuation constants in the stratified unbounded material for  $k_y = 0$  (excluding the lowest attenuation constant which is associated with the fundamental mode  $n=0$ ).

\*Author to whom correspondence should be addressed. engheta@ee.upenn.edu

- <sup>1</sup>A. Alù and N. Engheta, Phys. Rev. E **72**, 016623 (2005).
- <sup>2</sup>A. Alù and N. Engheta, Opt. Express **15**, 3318 (2007).
- <sup>3</sup>A. Alù and N. Engheta, Opt. Express **15**, 7578 (2007).
- <sup>4</sup>A. Alù and N. Engheta Phys. Rev. Lett. **100**, 113901 (2008).
- <sup>5</sup>M. G. Silveirinha, A. Alù, and N. Engheta, Phys. Rev. E **75**, 036603 (2007).
- <sup>6</sup>J. B. Pendry, D. Schurig, and D. R. Smith, Science **312**, 1780 (2006).
- <sup>7</sup>U. Leonhardt, Science **312**, 1777 (2006).
- <sup>8</sup>D. Schurig, J. J. Mock, B. J. Justice, S. A. Cummer, J. B. Pendry, A. F. Starr, and D. R. Smith, Science **314**, 977 (2006).
- <sup>9</sup>G. W. Milton and N. A. Nicorovici, Proc. R. Soc. London, Ser. A **462**, 3027 (2006).
- <sup>10</sup>W. Cai, U. K. Chettiar, A. V. Kildishev, and V. M. Shalaev, Nat. Photonics **1**, 224 (2007).
- <sup>11</sup>W. Cai, U. K. Chettiar, A. V. Kildishev, and V. M. Shalaev, Opt. Express **16**, 5444 (2008).
- <sup>12</sup>C. F. Bohren and D. R. Huffman, *Absorption and Scattering of Light by Small Particles* (Wiley, New York, 1983).
- <sup>13</sup>M. A. Ordal, Robert J. Bell, R. W. Alexander, Jr., L. L. Long, and M. R. Querry, Appl. Opt. **24**, 4493 (1985).
- <sup>14</sup>L. Brillouin, *Wave Propagation in Periodic Structures*, 2nd ed. (Dover, New York, 1953).
- <sup>15</sup>W. G. Spitzer, D. Kleinman, and D. Walsh, Phys. Rev. **113**, 127 (1959).
- <sup>16</sup>A geometry that may somehow resemble the one suggested here has been recently proposed to achieve cloaking at optical frequencies (Ref. 11). However, despite some apparent geometrical similarities, the cloaking technique, the material parameters, and the physical behavior of the cloak presented here are completely different than those presented in Ref. 11. Moreover, the two cloaks work for two different (orthogonal) polarizations of the electromagnetic wave.
- <sup>17</sup>CST Microwave Studio™ 5.0, CST of America, Inc., www.cst.com
- <sup>18</sup>M. G. Silveirinha, IEEE Trans. Antennas Propag. **54**, 1766 (2006).
- <sup>19</sup>P. A. Belov and C. R. Simovski, Phys. Rev. B **73**, 045102 (2006).
- <sup>20</sup>G. D. Mahan and G. Obermair, Phys. Rev. **183**, 834 (1969).
- <sup>21</sup>C. A. Mead, Phys. Rev. B **17**, 4644 (1978).